The Pulse Coupled Phasor Measurement Units

Lorenzo Ferrari, Reinhard Gentz, Anna Scaglione, Masood Parvania
Department of Electrical and Computer Engineering, University of California, Davis, CA, USA

***Abstract*—We propose a cross-layer sensor network architecture to convert measurements acquired by a population of sampling devices, into synchronous sensor array measurements, using a network synchronization protocol that is inspired by the dynamics of pulse coupled oscillators (PCO). We study the specific application of these sensors in the distribution section of the Smart Grid as low cost Phasor Measurement Units, that we refer to as the Pulse Coupled PMUs (PC-PMUs). The paper studies the impact of synchronization error on the quality of the phasor measurements analytically and via numerical simulations, considering a solution in which sensing and synchronization signals are both over the power-line medium. The analysis is valid for generic networks where the connectivity is radial, and the numerical results are carried on a 33-bus test network representing a typical distribution feeder.**

I. Introduction

Data acquisition is ubiquitous in Industrial Control Systems (ICS), and it consists of the regular sampling of analog measurements as well as digital variables, recorded by field devices and programmable logic controllers. Some ICS applications are particularly time sensitive: they require accurate time-stamping of information from the sensors so that the absolute time of their acquisition can be determined. The typical ICS solution to provide accurate timing is based on using a GPS-Receiver either directly on the sensor, or indirectly through a network that distributes accurate GPS time information using a clock distribution protocol, such as the Precision Time Protocol (PTP) [1]. GPS-Signals can be spoofed [2], and PTP protocols are not immune to cyber-attacks.

Synchronous sampling is particularly crucial in the power grid. In fact, time information is used to extract coherently the phase and amplitude of the AC carrier voltage and current across the grid. Sensors that perform this operation are called Phasor Measurement Units (PMUs), and their importance stems from the fact that they directly measure the system state variables, i.e. the voltage phasors. The use of a new class of synchro-phasors designed specifically for monitoring the distribution system state is currently under investigation in the US and such sensors are believed to potentially play an important role, as distributed generation, storage devices and electric vehicles are transforming power distribution systems into active systems with two-way power flows.

In this paper, we propose a novel design concept for syncro-phasors measurements that could lead to a viable and economic solution for widespread deployments in the distribution grid. The new idea lies in using a protocol inspired by the Pulse Coupled Oscillator (PCO) model [3], [4], as the primitive for obtaining coherent phasor measurements. We refer to our architecture as the Pulse Coupled Phasor Measurements Units (PC-PMUs). Compared to other techniques, PCO is a cross-layer communication scheme, which is therefore capable of reducing timing errors to the limits that are present at the physical layer and it is very scalable. The idea of using algorithms inspired by the PCO model for wireless network synchronization was proposed, analyzed and implemented in a number of previous papers [5]–[12]. However, to the best of our knowledge, the idea of using a PCO technology to obtain coherent sensors' sampling is new, and so is its specific application to the development of cost effective PMUs. The key-factor that makes this kind of implementation economically convenient is the possibility to integrate on a single chip the synchronization signal, the sensor and the radio with a unique architecture. In addition to this, a dedicated private channel for synchronization guarantees an higher security of the system from potential cyber attacks compared to the public and easily accessible GPS signal. The proposed PC-PMU network architecture works irrespective of the choice of medium for communications. Here, however, we envision that the PC-PMU would use the power-line for the dual purpose of sensing as well as communicating with the other measurement sites. Specifically, while the spectrum between 0 and 120Hz is sampled synchronously to obtain the phasor data, we assume that the synchronization signals of the PC-PMUs occupy the band 250-350 kHz, which is used in half-duplex. Therefore, we choose bandwidth, noise and path loss parameters that are consistent with communications on such band over a distribution network. In our analysis, we consider errors in estimating arrival time and propagation delays which were neglected previous studies [4], [6] and analyze the accuracy of the synchro-phasor estimation in a distribution network with a radial structure.

The paper is organized as follows: in Section II we review the PCO synchronization scheme and describe the sources of synchronization errors. In Section III we describe the PC-PMU sensor architecture. In Section IV, we study the convergence of the PCO protocol, in Section V, we evaluate the performance of our system, validated numerically in Section VI.

II. The PCO Protocol

Pulse Coupled Oscillators (PCO) were first introduced in mathematical biology to model pace maker cells [3] and later were analyzed in [4]. All PCO based algorithms work based on having the network agents perform announcements when a local timer expires and updating the timer when such announcements are received. The announcements consists of transmitting of a common *beacon* signal that does not identify the node in any way, every time a local PCO timer expires (*the firing event*). All counters have the same frequency and we normalize their period T to be 1. If at time t node i performed $k_{i,t}$ updates, the timer is:

$$\Phi_i(t) = (t - \Phi_i[k_{i,t}]) \pmod T, \quad i = 1, \dots, N \qquad (1)$$

where $\Phi_i[k_{i,t}] \in [0, T)$ denotes the misalignment of the timers with respect to a virtual global reference. To synchronize node

i only relies on observing its local clock state $\Phi_i(t)$ and modifying it based on its clock state value at the times when node i detects other nodes firing signals.

In decentralized PCO synchronization protocols, the ultimate objective is to align all timers to expire concurrently, which means synchronization. Firing and detection cannot occur concurrently (the communication is half-duplex). Therefore, if there are no transmission delays, firing in unison is a fixed point. There are several possible variations of the PCO synchronization in biological systems [3]; they effectively reflect the physical mechanisms used to implement the timers. However, for the purpose of synchronizing a network using a micro-controller the algorithm in [13], which assumes that $\Phi_i(t)$ is a timer updated by a local clock with period much smaller than T, is the simplest. Let assume that node i's timer expires at time t_i and sends out the firing beacon through the network. Then, all the recipient nodes j receiving this beacon, perform the following update:

$$\Phi_j(t_i^+) = \begin{cases} \min\{(1+\alpha)\Phi_j(t_i), 1\} & \text{if } \rho < \Phi_j(t_i) < 1 \\ \Phi_j(t_i) & \text{else} \end{cases} \tag{2}$$

where $\alpha > 0$ is a constant, ρ indicates the refractory period that, as acknowledged in previous papers [6], [14], strengthens the convergence of the protocol and the phase Φ_j is normalized over T. If the result of (2) is 1 then node j fires immediately and it is then synchronized to node i. In a complete network the two nodes will continue to fire at unison from this point on, and these events are called *absorptions* in [4]. Each absorption is permanent in a fully connected network but it is not in a locally connected network. In spite of that, after sufficient number of updates as in (2), time synchronization is achieved in any connected network. An upper bound on the number of updates needed for convergence is given in [15]. PCO synchronization methods work with all network topologies that are connected, however the convergence speed depends on the graph connectivity. In Section IV we characterize the synchronization accuracy obtainable under realistic propagation models for a tree network. In section V we analyze the impact of timing error on the quality of the PMU measurements.

The rate of convergence of the PC-PMU sensors on different graph sizes and topologies is going to be investigated in future work. Next we briefly describe the PC-PMU.

III. The PC-PMU sensor architecture

The PC-PMU is a sensor as well as a very simple radio devoted to sending and receiving firing signals used to synchronize the sensor network. A sketch of the device is shown in Fig. 1. A key element of the design is the use of a common stable oscillator to advance the PCO timer, control the radio portion of the PC-PMU and, at the same time, to advance the sampling epochs of the PMU portion, that samples the complex envelope of the power carrier. Sharing this clock guarantees that physical events in the PCO protocol radio are directly tied with the samples acquired in the PMU portion of the sensor. Under ideal synchronization conditions sensor measurements that belong to the same PCO timer iteration are taken synchronously at all platforms.

In Fig. 1 we assume (this is not a restriction) that sensing and communications both use the power line medium. Hence,

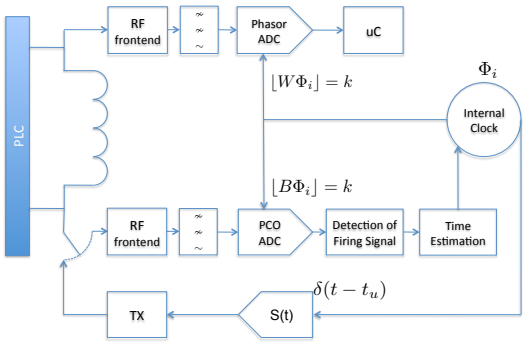

Fig. 1. Pulse Coupled Phasor Measurement Unit

the analog front end over the power line carrier splits the signal using two filters: 1) a PMU filter; 2) a PCO synchronization filter, with bandwidth approximately equal to the baud-rate B and centered around a much higher carrier, used for the transmission and reception of firing signals over the same medium. At both sides the receivers extract the corresponding complex envelopes. The PCO branch is used half-duplex to detect and estimate the arrival time of firing signals through a filter matched to the firing signal, and to transmit the firing signal when the PCO timer expires. Specifically, at times t_i such that $\Phi(t_i) = 1$ node i sends the RF signal $\Re\{s(t - t_i)e^{j\omega_s t}\}$, where $s(t)$ is the envelope of the firing signal. The latter has bandwidth approximately equal to B and duration much smaller than the PCO period. $s(t)$ is a pseudo-noise signature, optimized to provide sufficient processing gain and a peaky autocorrelation function.

The PMU section is coupled to the power line to extract a signal proportional AC power carrier voltage (and current) at a certain bus where the PC-PMU is deployed. The power carrier is a narrowband signal centered around 50 or 60 Hz:

$$v(t) = \Re\{|V(t)|e^{j(\omega_0 t + \theta_V(t))}\}. \tag{3}$$

Given the modest bandwidth of interest for the PMU signal a good choice is to use an anti-aliasing filter with cutoff frequency $W = 2\omega_0/\pi$ i.e. four times the nominal frequency, and then sample the bandpass signal to extract the complex envelope digitally, potentially filtering a narrower spectrum around ω_0.

The PCO timer and radio advance at a rate B approximately equal to the bandwidth of the firing signals. We consider $B \gg W$ and that their ratio is an integer $B/W = Q$. The higher frequency B is used to advance the PCO clock $\Phi_i(t)$, and every Q sub-intervals (corresponding to samples of the PCO transmitter or receiver) a new PMU sample in generated. The number of PMU samples per period is equal $L = WT$ and if we use the normalization $T = 1$ for time $L = W$. The difference in time scales between the operations of the synchronization radio and the phasor sampling can improve the accuracy of the phasor measurements.

Note the PC-PMU architecture here does not include a modem to transmit the sensor readings, but it can be easily integrated with other communication platforms that fit the purpose. Given the relatively low duty cycle of the PCO firing events it is not even unreasonable to use the same power line

carrier concurrently, as the interference from the PCO activities could be limited, especially if the radio can be activated at times that do not overlap with the steady state PCO firing activity, which has a highly predictable pattern.

IV. PCO UNDER REALISTIC PROPAGATION MODELS

In the presence of transmission delays, the PCO update is modified so that the nodes ignore any firing that occurs within a *refractory period* after their own firing event. Such *refractory period* (used also in the original Peskin model [3]) is set to be an upper-bound for the unknown and deterministic portion of the delay between the firing epoch and its detection.

While the propagation delay and the duration of the firing signal contribute to an offset that is bounded and deterministic, the PC-PMU receiver observes a signal that has limited energy and bandwidth and is embedded in noise. Assuming that the arrival time of firing signals is provided by an unbiased estimator, the firing time of node i recorded at node j is affected by an additional random error. Hence, the PCO timer that node j will read at the time it estimated the firing of node i happened is given by:

$$\Phi_j(\hat{t}_i) = \Phi_j(t_i) + \tau_{(i,j)} + e_j(t_i) \tag{4}$$

where t_i and $\hat{t}_i$ are the transmitting/receiving times, $\tau_{(i,j)}$ is propagation delay and $e(t_i)$ is the time estimation error. We assume that $\tau_{(i,j)} = \tau_{(j,i)}$. The node update will then be

$$\Phi_j(\hat{t}_i^+) = \min\left\{(1+\alpha)\Phi_j(\hat{t}_i), 1\right\} \tag{5}$$

$$= \min\left\{(1+\alpha)\Phi_j(t_i) + \tau_{(i,j)} + e_j(t_i), 1\right\}. \tag{6}$$

We model the distribution of $e_j(t_i)$ as $\mathcal{N}(0, \sigma_j^2)$, with σ_j^2 equal to the Cramer-Rao-Bound for time estimation in Gaussian white noise, which we assume is achieved by the receiver estimator (see e.g. [16] Ch.3):

$$\sigma^2 \geq (SNR_{(i,j)} \cdot \bar{F^2})^{-1} \tag{7}$$

Here $SNR_{(i,j)}$ is the signal-to-noise-ratio (the ratio of the received energy of the firing signal from node i to node j divided by the receiver j noise spectral density) and $\bar{F^2}$ is the mean square bandwidth of the firing signal envelope $s(t)$:

$$\bar{F^2} = \frac{\int_{-\infty}^{\infty}(2\pi f)^2|S(f)|^2 df}{\int_{-\infty}^{\infty}|S(f)|^2 df} \tag{8}$$

where $S(f)$ is the Fourier transform of the firing signal envelope $s(t)$. In the presence of delays and with refractory period, the nodes are considered *synchronized* if their timers are within a refractory period of their neighbors. Because the Gaussian distribution is unbounded, no choice for a finite refractory period can, in principle, guarantee that the synchronization condition will be maintained with probability one. In practice, events in which one or more nodes escape from the fixed point set can be made arbitrarily rare, but the important difference to take into account is that these errors can be positive or negative. Hence, the receiver will need to have a refractory period that includes a portion of time prior to the node own firing, to account for errors that may place the firing event detected even before it actually occurred. Note that, assuming that a lower bound $\tau_{min} \leq \tau_{(i,j)}$ is known at each node, in updating the PCO timer the node can compensate for this delay τ_{min} and therefore, we consider from now on $\tau_{(i,j)}$ as the unknown residual delay compared to τ_{min}.

In our numerical analysis the CRB that characterize most links is very small compared to the propagation delay. Hence, the PMU measurement error is dominated by the unknown bias in the estimate that is due to the propagation delay. Next we neglect the time estimation error due to noise and characterize the fixed point of the PCO protocol considering the effect of unknown propagation delays.

A. Fixed points for the PCO timers with propagation delays

The states of the PCO clocks can be represented with circles that move clockwise like clock dials, to complete the cycle of duration T, and jump by the amount in (9) whenever they register the firing of a neighbor. Our goal in this section is to study the fixed points for the algorithm, for the *noiseless case*, in which $e_j(t_i) = 0$ for a communication network with a tree topology.

Each node fires when it reaches the end of its clock. A receiving node j, if we neglect the estimation error $e_j(t_i)$, updates its own phase only after a time equal to the unknown propagation time between them:

$$\Phi_j(t_i^+ + \tau_{(i,j)}) = \begin{cases} \min\left\{(1+\alpha)(\Phi_j(t_i) + \tau_{(i,j)}), 1\right\} \\ \text{if } \rho < \Phi_j(t_i) + \tau_{(i,j)} < 1 \\ \Phi_j(t_i + \tau_{(i,j)}) \\ \text{if } 0 < \Phi_j(t_i) + \tau_{(i,j)} \leq \rho. \end{cases} \tag{9}$$

When the result of the update described in (9) is equal to 1 (i.e. when first $(1+\alpha)(\Phi_j(t_i) + \tau_{(i,j)}) \geq 1$), then node j fires immediately and resets its phase to 0. Note that, at the same time, the timer value of the firing node i is:

$$\Phi_i(t_i^+ + \tau_{(i,j)}) = \Phi_i(t_i^+) + \tau_{(i,j)} = 0 + \tau_{(i,j)} = \tau_{(i,j)}$$

which means that the difference between node j PCO timer and of node i at the update time is exactly the signal travel time $\tau_{(i,j)}$ from i to j. The *absorption* is generally not permanent in a locally connected network, though eventually all nodes are absorbed. Let us introduce the vector of *phase differences* between nodes i and j at time t as

$$\Delta\Phi_{(i,j)}(t) = \Phi_i(t) - \Phi_j(t) \pmod 1 \tag{10}$$

We introduce $L_{(i,j)}$ as the set of edges on the shortest path from node i to node j. From (9) we can directly prove the following result:

Proposition 1. *Consider a tree network, in which each link has delay $\tau_{(i,j)}$ and nodes can hear only their immediate neighbors. Fixed points for the PCO algorithm are $\mathbf{\Phi}(t)$ such that there is a node firing first, that we call head node, with index h, and all other nodes have a timer offset with respect to the head node equal to:*

$$\Delta\Phi_{(i,h)}(t) = \sum_{(k,m)\in L_{(i,h)}} \tau_{(k,m)}, \tag{11}$$

which is the propagation delay over the shortest path connecting node i and the head node h.

If we set the refractory period $\rho > 2max_{i,j}\{\tau_{(i,j)}\}$ we can neglect "echoes", i.e. the firing of a neighbor in reaction to

our firing. Then it is clear that nodes are trapped in states like (11), as already noticed in [14]. It is not as obvious that these are the only fixed points; a sketch of a proof is given in the Appendix.

V. Phasor Measurement Error Model

We assume that the PC-PMU clocks have negligible frequency offsets and that the phasor measurement noise is negligible. Under these approximations, in this section we analyze the impact of a relative time error in the acquisition of samples of the voltage phasors of the power carrier (analogous equations can be written for the current phasors). Let t_0 be a generic sampling epoch, and $t_0 + \Delta\Phi$ be the actual time the sample is taken. If the envelope variations are negligible during the interval $\Delta\Phi$, the sample of the AC signal will be

$$v_i(t_0 + \Delta\Phi) \approx \Re\{|V_i(t_0)|e^{j(\omega_0 t_0 + \omega_0 \Delta\Phi_i(t_0) + \theta_{V_i}(t_0))}\} \quad (12)$$

and, therefore, after the extraction of the phasor (which we assume to work ideally), the effect of timing error can be modeled as a phase rotation of the envelope:

$$\widehat{V}_i(t_0) \approx |V_i(t_0)|e^{j(\theta_{V_i}(t_0) + \omega_0 \Delta\Phi_i(t_0))} \quad (13)$$

where $\Delta\Phi_i(t_0)$ is the time offset with respect to an arbitrary reference node:

$$\Delta\Phi_i(t_0) = \Phi_i(t_0) - \Phi_r(t_0). \quad (14)$$

If, without loss of generality, we assign node 1 as the reference node for the entire network we have measurements:

$$\widehat{\mathbf{V}}(t_0) = \left[\widehat{V}_1(t_0), \widehat{V}_2(t_0 + \Delta\Phi_2), ..., \widehat{V}_N(t_0 + \Delta\Phi_N)\right]$$

where $\Delta\Phi_i = \Phi_i(t_0) - \Phi_1(t_0)$ (for $i = 2, 3, ..., N$) represents the misalignment of the internal PCO clocks.

Let $\mathbf{e}(\Phi) = (1, e^{j\omega_0\Delta\Phi_2}, \ldots, e^{j\omega_0\Delta\Phi_N})$ and:

$$\mathbf{\Delta}(\Phi) = diag(\mathbf{e}(\Phi)). \quad (15)$$

Omitting the time index t_0, it follows from (13) that the Mean Square Error (MSE) is:

$$\mathbb{E}\{||\mathbf{V} - \hat{\mathbf{V}}||^2\} = \mathbb{E}\{||(\mathbf{I}_N - \mathbf{\Delta}(\Phi))\mathbf{V}||^2\} = \\ = \mathbf{V}^H \mathbb{E}\left\{(\mathbf{I}_N - \mathbf{\Delta}(\Phi))^*(\mathbf{I}_N - \mathbf{\Delta}(\Phi))\right\}\mathbf{V}$$

Now the product $(\mathbf{I}_N - \mathbf{\Delta}(\Phi))^*(\mathbf{I}_N - \mathbf{\Delta}(\Phi))$ is a diagonal matrix, with identical diagonal entries in position i and $i+N$, for $i = 1, \ldots, N$ and that can be approximated as follows:

$$\{(\mathbf{I}_N - \mathbf{\Delta}(\Phi))^*(\mathbf{I}_N - \mathbf{\Delta}(\Phi))\}_{i,i} = |1 - e^{j\omega_0\Delta\Phi_i}|^2 \approx \omega_0^2\Delta\Phi_i^2. \quad (16)$$

This leads to the MSE final expression:

$$\mathbb{E}\{||\mathbf{V} - \hat{\mathbf{V}}||^2\} \approx \omega_0^2 \mathbf{V}^H \mathbb{E}\{\mathbf{\Delta}^2(\Phi)\}\mathbf{V} \\ = \omega_0^2 \sum_{i=1}^{N} \mathbb{E}\{\Delta\Phi_i^2\}|V_i(t_0)|^2. \quad (17)$$

In order to evaluate $\mathbb{E}\{\Delta\Phi_i^2\}$ we need to characterize the statistics of $\Delta\Phi_i$. Let the vector $\mathbf{p} = [p_1, p_2, ..., p_N]$ with p_i representing the probability that node i is the *head* node. In light of Proposition 1:

$$\mathbb{E}\{\Delta\Phi_i^2\} = \sum_{h=1}^{N} p_h \left(\sum_{(k,m)\in L_{(i,h)}} \tau_{(k,m)} \right)^2 \quad (18)$$

which, when substituted in (17), provides an analytical expression for the MSE as a function of $\mathbf{p}$. Note the mean $\mathbb{E}\{\Delta\Phi_i\}$ has a very similar expression: one simply does not have to raise to the power of 2 the sum path delay.

The characterization of the vector $\mathbf{p}$ is non-trivial and beyond the scope of this work. Next, we provide a semi-analytical solution, by evaluating $\mathbf{p}$ via numerical simulations of the PCO algorithm under many initial conditions. The simulations show clearly that $\mathbf{p}$ depends not only on the connectivity of the graph but also on the distances between nodes and the coupling factor α in the update equation (2).

VI. Simulation Results

In our numerical analysis we considered PC-PMU sensors deployed at all buses of the sample 33-bus distribution feeder [17] in Fig. 2. Lacking information about the actual physical distances among nodes, we assumed a particular inductance per unit length and used the information about the line admittance to estimate the transmission lines lengths. We considered a central frequency of 300 kHz with a bandwidth equal to 100kHz, we set the transmission time at 20 μs and we considered a loss coefficient of $40dB/km$. The results were compared with (17), and (18). We ran the PCO algorithm over 960 Monte Carlo trials, with random initial phases, until it reached a fixed point and then we transferred the phase errors obtained onto the voltage phasor samples calculated using MATHPOWER in order to generate "realistic" voltage phasors, and evaluate the error. We considered various other loads conditions intervals of 5 minutes along a period of 24 hours but the results remained almost unchanged with respect to the state value.

The frequency with which each node is the *head* node is shown in Fig.3. As expected, nodes with higher degree appear to have higher p_i while the smallest probability mass of being head is for nodes with only one neighbor.

In the presence of time estimation error $e_j(t_i)$ due to noise, in choosing the refractory period one is confronted with a trade-off between attaining stable synchrony and increasing the speed of convergence. The effect of this choice will also be the subject of future work; for this simulation has been set to 10^{-4}. Fig. 4 shows the numerical simulation of the MSE versus the PCO signal transmission power, normalized towards the number of sensors because, even if we are not able to place a PMU in every bus, we can still place just a

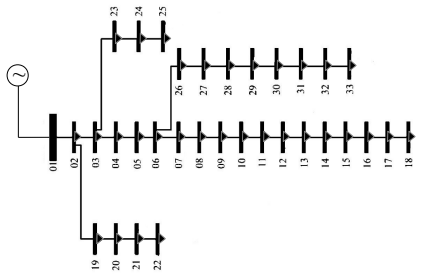

Fig. 2. The sample 33-bus distribution feeder [17]

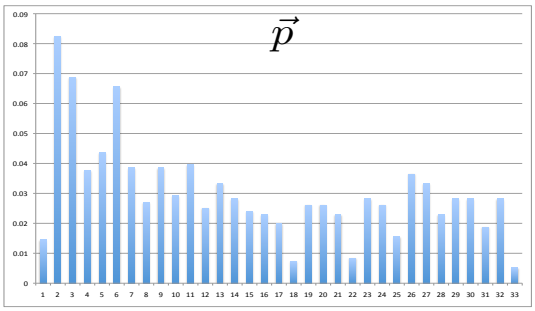

Fig. 3. Histogram of frequency for each node being the *head* node

PCO sensor to keep synchronization among non-adjacent buses (the simulation considers PMUs in every bus). However, our analysis suggests that reducing the number of PCO nodes does not modify the worst case in terms of phase difference but reduces the probability of a central node to be the *head* node [14] and so it worsens the average accuracy we can get. We can see that the measurement error is not significantly increased by the presence of noise in the firing time estimate. Since we modeled each error in arrival time as $e_j(t_i) \sim \mathcal{N}(0, \sigma^2)$ we can directly add its variance to the variance of $\Delta\Phi_i^2$. Our analysis, provides a close lower bound for the actual performance. The gap observed is reasonable, considering the approximation made in (16). We also noted that, occasionally, the noise brings a slight benefit, reducing the timing offsets below the $\tau_{(i,j)}$. We see that we need a minimum power around 20 dBm to reach a good match between simulation and estimation. This is expected, as $e_j(t_i)$ becomes negligible compared to the $\tau_{(i,j)}$s. We also show how our figure of merit

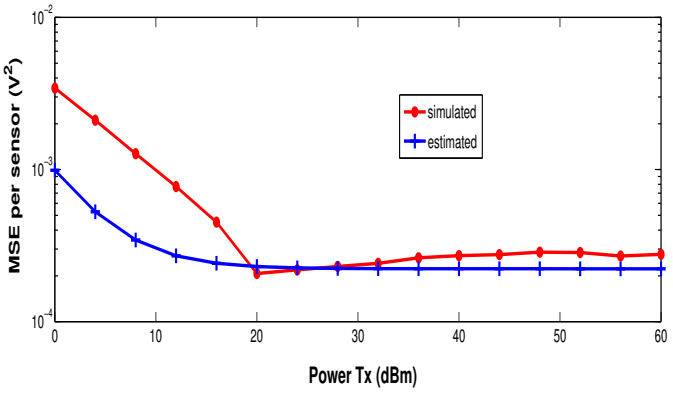

Fig. 4. Simulation and Estimation of the Mean Square Error in measurement changing the transmitted power

VII. Conclusions and Future Work

We have introduced a completely new device, the PC-PMU, aimed at producing low cost PMUs for the Smart Grid. We analyzed its accuracy taking into account the non-ideal synchronization conditions. The analysis has been developed for radial distribution system but it is extendable to transmission systems: future work is going to examine more complex effects and network configurations where the non-trivial compensation for propagation delays becomes mandatory.

Appendix

Proof of Lemma 1 – Considering an initial ordering of the PCO phases, in a fully connected network nodes cannot switch their relative position. They can do so in a locally connected network, where a node j that is within the refractory period compared to node i timer, can be pulled away from it by a neighboring node k that is not in neighbor of node i.

To validate our proposition we consider a three node network (Fig. 5) from which we extrapolate the general result. What we show is that eventually the nodes settle in a certain relative ordering and when they do they ought to be in the configuration in Proposition 1. To analyze the case in Fig. 5 we use the same algebraic model introduced in [13]. Let us assume without loss of generality that $(\Phi_1 > \Phi_2 > \Phi_3)$. Let $\Delta_1(t) = \Phi_1(t) - \Phi_2(t) \pmod 1$, $\Delta_2(t) = \Phi_2(t) - \Phi_3(t) \pmod 1$, and $\Delta_3(t) = \Phi_3(t) - \Phi_1(t) \pmod 1$. Assume that α is such that there are no absorptions in round R, that is the result of $\Phi_j(t_i + \tau_{(i,j)}) = \min\left\{(1+\alpha)(\Phi_j(t_i) + \tau_{(i,j)}), 1\right\} < 1 \quad \forall i, j$. Suppose that node 1 fires first round $R = 1$, at time t_1. Only node 2 updates its phase and if we consider $t_1^+ = t_1 + \tau_{(1,2)}$, $\Phi_1(t_1^+) = \tau_{1,2}$. Based on the update rule given in (9) we have:

$$\begin{aligned}
\Delta_1(t_1^+) &= \tau_{(1,2)} + 1 - \Phi_2({t_1}^+) \\
&= \tau_{(1,2)} + 1 - (1+\alpha)(1 - \Delta(t_1) + \tau_{(1,2)}) \\
&= (1+\alpha)\Delta_1(t_1) - \alpha(1 + \tau_{(1,2)}) \\
\Delta_2(t_1^+) &= (1+\alpha)(\Phi_2(t_1) + \tau_{1,2}) - (\Phi_3(t_1) + \tau_{(1,2)}) \\
&= -\alpha\Delta_1(t_1) + \Delta_2(t_1) + \alpha(1 + \tau_{(1,2)}) \\
\Delta_3(t_1^+) &= \Delta_3(t_1)
\end{aligned}$$

At time t_2, node 2 fires but nodes 1 and 3 hear at different times, so assuming $\tau_{(2,3)} > \tau_{(1,2)}$ and $t_2^+ = t_2 + max\{\tau_{(1,2)}, \tau_{(2,3)}\}$ we can write:

$$\begin{aligned}
\Delta_1(t_2^+) &= (1+\alpha)\Delta_1(t_2) + \alpha\tau_{(1,2)} \\
\Delta_2(t_2^+) &= (1+\alpha)\Delta_2(t_2) - \alpha(1 + \tau_{(2,3)}) \\
\Delta_3(t_2^+) &= (1+\alpha)\Delta_3(t_2) - \alpha(\tau_{(1,2)} - \tau_{(2,3)})
\end{aligned}$$

Finally, at time t_3, node 3 fires and we have

$$\begin{aligned}
\Delta_1(t_3^+) &= \Delta_1(t_3) - \alpha\Delta_2(t_3) - \alpha(1 + \tau_{(2,3)}) \\
\Delta_2(t_3^+) &= (1+\alpha)\Delta_2(t_3) + \alpha(1 + \tau_{(2,3)}) \\
\Delta_3(t_3^+) &= \Delta_3(t_3)
\end{aligned}$$

Now, we can define:

$$\begin{aligned}
\widehat{\Delta}_1(t) &= \Delta_1(t) - \tau_{(1,2)} \pmod 1 \\
\widehat{\Delta}_2(t) &= \Delta_2(t) - \tau_{(2,3)} \pmod 1 \\
\widehat{\Delta}_3(t) &= \Delta_3(t) + \tau_{(1,2)} + \tau_{(2,3)} \pmod 1
\end{aligned}$$

and, with a few simplifications we can express $\widehat{\mathbf{\Delta}}(t_3^+)$ as a function of $\widehat{\mathbf{\Delta}}(t_1)$ in order to describe the evolution of our 3-node system in each complete round of firing events:

$$\widehat{\mathbf{\Delta}}[R+1] = M\widehat{\mathbf{\Delta}}[R] + \mathbf{v} \tag{19}$$

Fig. 5. A 3-node example

where

$$\mathbf{M} = \begin{bmatrix} (1+\alpha)(\alpha^2+\alpha+1) & -\alpha(1+\alpha) & 0 \\ -\alpha(1+\alpha)^2 & (1+\alpha)^2 & 0 \\ -\alpha & -\alpha & 1 \end{bmatrix} \quad (20)$$

and

$$\mathbf{v} = \begin{bmatrix} -\alpha(\alpha^2+\alpha+2(1-\tau_{(1,2)}+\tau_{(2,3)})) \\ \alpha(\alpha^2+\alpha+1+2\tau_{(2,3)}) \\ \alpha+(1-2\alpha)\tau_{(1,2)}+\tau_{(2,3)} \end{bmatrix} \quad (21)$$

We remind that $\sum_i \widehat{\Delta}_i = 1$ and $\forall i \quad 0 \leq \widehat{\Delta}_i \leq 1$, and since the sum of each column of $\mathbf{M}$ is equal to 1 and the eigenvector 1 has only one feasible eigenvector equal to $\widehat{\mathbf{\Delta}}_\infty = [0,0,1]^T$. Since $\mathbf{v}$ is constant and positive $\left(||\mathbf{v}||_1 = \tau_{(1,2)} + \tau_{(2,3)}\right)$ and $||\widehat{\mathbf{\Delta}}||$ has to be always equal to 1, $\widehat{\mathbf{\Delta}}_\infty = [0,0,1]^T$ represents our only possible convergence point, and so:

$$\begin{aligned} \Delta_1(t) &= \tau_{(1,2)} \\ \Delta_2(t) &= \tau_{(2,3)} \\ \Delta_3(t) &= 1 - (\tau_{(1,2)} + \tau_{(2,3)}) \end{aligned}$$

The proof holds if the firing order of the nodes does not change, but this can happen in a locally connected scenario. However, it has been observed many times before that the probability of switching order eventually converges to 0 for networks that are connected. We again illustrate this for the case of three nodes and, for the sake simplicity, here we ignore the propagation delay. Let node 1 fire first at time t_1. If $(1+\alpha)\Phi_2(t_1) > \Phi_3(t_1)$ and $\Phi_2(t_1) < \Phi_3(t_1)$ we have a change in position; then node 2 fires and, when node 3 fires, it is possible to have again a switch between node 1 and node 2. We can derive the condition that would allow that to happen, considering the update rule and the elapsed time. We have a second switch if:

$$(1+\alpha)^2\Phi_2(t_1) > \alpha\Phi_3(t_1) + \frac{\alpha^2+\alpha+1}{\alpha+1}.$$

It can be verified that this condition is more restrictive and if we order the inequalities:

$$\begin{aligned} \textit{I switch} \quad & \Phi_2(t_1) > \frac{1}{1+\alpha}\Phi_3(t_1) \\ \textit{II switch} \quad & \Phi_2(t_1) > \frac{\alpha}{(1+\alpha)^2}\Phi_3(t_1) + \frac{\alpha^2+\alpha+1}{(1+\alpha)^3} \end{aligned}$$

and since $\Phi_2(t_1)$ has to be lower than $\Phi_3(t_1)$ the oscillation of the firing order of the nodes is always eventually impossible, as the conditions on the phases to have more and more such switching become increasingly stringent. Thus, in general we can start from the state in which we have no change in order as our initial random condition to proof the convergence, following the steps previously indicated.

We can generalize our proof for an N-node tree network and verify that the PCO system always converges to a single node that we call *head*, that represents the first in the line, and all the others follow it spaced of their delay relative the previous node in the line connecting it with the head node.

That is because, in essence, every possible tree network fixed point can be built starting from the 3-node example (in Fig.5) and consecutively connecting one node at a time to an existing node of the system, say node *i*. In any case, three possible synchronization scenarios would happen: 1) the new node is absorbed by the node *i*, which would not affect the system; 2) the node *i* is absorbed by the new node and becomes the *head* node of the previous system which is preceded by the new node that is the *head* of the new whole system; 3) the node *i* goes on bouncing between the above two cases, meaning that the order of nodes is changed cyclically. However, as shown for the middle node in the 3-node example, this can happen with a monotonically decreasing probability. So the system always converges to one of the first two cases and this allows us to state the convergence for every tree network with N nodes.

REFERENCES

[1] "Ieee standard for a precision clock synchronization protocol for networked measurement and control systems," *IEEE Std 1588-2008 (Revision of IEEE Std 1588-2002)*, pp. c1–269, July 2008.

[2] T. Niels, P. Christina, R. Kasper, and C. Srdjan, "On the requirements for successful gps spoofing attacks," in *18th ACM conference*, 2011.

[3] C. Peskin, "Mathematical aspects of heart physiology," *Institute of Mathematical Sciences*, 1975.

[4] R. Mirollo and S. Strogatz, "Synchronization of pulse-coupled biological oscillators," *SIAM J. Appl. Math.*, vol. 50, no. 6, pp. 1645–1662, 1990.

[5] Y.-W. P. Hong and A. Scaglione, "Time synchronization and reachback communications with pulse-coupled oscillators for uwb wireless ad hoc networks," in *IEEE Conference on Ultra Wideband Systems and Technologies (UWBST 2003)*, 2003.

[6] R. Pagliari and A. Scaglione, "Scalable network synchronization with pulse-coupled oscillators," *IEEE Trans. Mobile Computing*, vol. 10, no. 3, pp. 392–405, 2011.

[7] X. Wang and A. Apsel, "Pulse coupled oscillator synchronization for communications in uwb wireless transceivers," in *MWSCAS*, 2007.

[8] A. Hu and S. Servetto, "On the scalability of cooperative time synchronization in pulse-connected networks," in *IEEE Transaction on Information Theory*, 2006.

[9] E. Mallada and K. Tang, "Synchronization of coupled oscillators," in *ITA*, 2010.

[10] A. Tyrrell, G. Auer, and C. Bettstetter, "Biologically inspired synchronization for wireless networks," in *Advances in biologically inspired information systems*, 2007.

[11] Z. An, H. Zhu, X. Li, C. Xu, Y. Xu, and X. Li, "Nonidentical linear pulse-coupled oscillators model with application to time synchronization in wireless sensor networks," *IEEE Trans. Industrial Electronics*, vol. 58, no. 6, pp. 2205–2215, June 2011.

[12] D. Lucarelli and I.-J. Wang, "Decentralized synchronization protocols with nearest neighbor communication," in *Sensys*, 2004.

[13] R. Pagliari, A. Scaglione, and Y. Hong, "Adaptive wireless networking primitives for distributed scheduling: Can radios swarm?" in *2009 3rd IEEE International Workshop on Computational Advances in Multi-Sensor Adaptive Processing (CAMSAP)*, pp. 133–136, 2009.

[14] A. Tyrrell, G. Auer, and C. Bettstetter, "On the accuracy of firefly synchronization with delays," in *Applied Sciences on Biomedical and Communication Technologies, 2008. ISABEL '08. First International Symposium on*, pp. 1–5, Oct 2008.

[15] S. Ashkiani and A. Scaglione, "Pulse coupled discrete oscillators dynamics for network scheduling," in *Proc. 2012 50th Annual Allerton Conference on Communication, Control, and Computing (Allerton)*, pp. 1551–1558, 2012.

[16] S. M. Kay, *Fundamentals of Statistical Signal Processing*. Prentice Hall, 1993.

[17] A. A. Algarni and K. Bhattacharya, "A generic operations framework for discos in retail electricity markets," *IEEE Trans. Power Systems*, vol. 24, no. 1, pp. 356–367, 2009.